Bruface
Brussels Faculty of Engineering

ULB

UNIVERSITÉ LIBRE DE BRUXELLES

Communication Channel Finite-Difference Time Domain

DIALLO Mouhammadou

MUKENDI TSHISUAKA Gael

FASSI FIHRI Ilias Kacem

Professor
DE DONCKER Philippe

Assistants
DERENNE Sullivan
LEMAIRE Thomas

Academic Year
2015 - 2016

Contents

1 Introduction

The purpose of this project is to implement a method in order to numerically solve Maxwell's equations. Hereafter we will define and analyze a set of simulations that illustrate some phenomena of electromagnetics.

2 The 1D FDTD algorithm

In this this section, the 1D FTDT is derived in order to see how the method works. The 2D implementation will be done in the next section.

In electromagnetic, two principal equations are of interest. They are the well-known Maxwell equations:

$$\begin{aligned} \frac{\partial \vec{E}}{\partial t} &= \frac{1}{\epsilon} \nabla \times \vec{H} \\ \frac{\partial \vec{E}}{\partial t} &= -\frac{1}{\mu} \nabla \times \vec{E} \end{aligned} \tag{1}$$

The goal of the Finite-Difference Time-Domain is solve numerically these equations by approximating the derivatives in (1) and (2) with finite differences.

The derivatives is thus replaced by the formula:

$$f'(x_o) \approx \frac{f\left(x_o + \delta/2\right) - f\left(x_o - \delta/2\right)}{\delta} \tag{2}$$

These main machinery of the FDTD is based on the Yee Algorithm, which consist to:

1. Replace the derivatives in (1) and (2) with finite difference by discretizing space and time
2. Evaluate the magnetic field one time-step into the future
3. Evaluate the electric field one time-step into the future
4. Repeat the previous two steps

In one-dimensional space, the equation (1) and (2) can be written as:

$$\begin{aligned} \frac{\partial E_z}{\partial t} &= \frac{1}{\epsilon}\frac{\partial H_y}{\partial x} \\ \frac{\partial H_y}{\partial t} &= \frac{1}{\mu}\frac{\partial E_z}{\partial x} \end{aligned} \tag{3}$$

The discretization of the latter is required to apply step 1. We have:

$$\begin{aligned} E_z(x,t) = E_z(a\Delta x, b\Delta t) = E_z^{a,b} \\ H_y(x,t) = H_y(a\Delta x, b\Delta t) = H_y^{a,b} \end{aligned} \tag{4}$$

where Δx design the spatial step and Δt the time step. Figure 2 describes the different space-time locations of the fields. It can be seen that there is an offset of $\frac{1}{2}$ between E_z and H_y which are used to discretize the red dot.

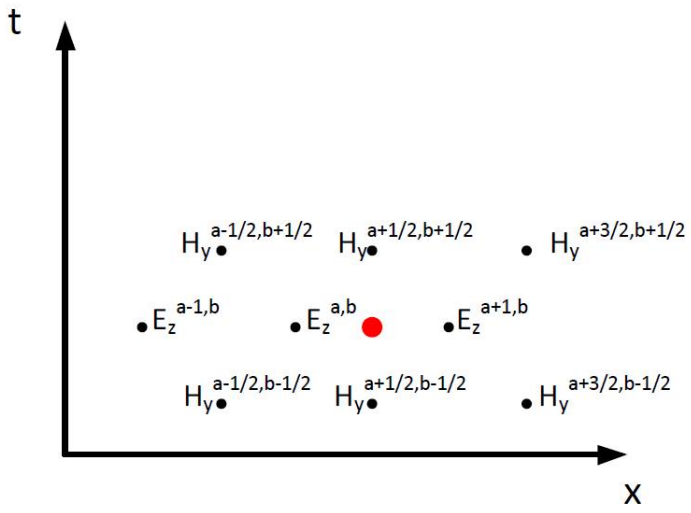

Figure 1: Discretization and space-time location

The update of equations for H_y and E_z are then given by:

$$\begin{aligned} H_y^{a+1/2,b+1/2} &= H_y^{a+1/2,b-1/2} + \frac{\Delta t}{\mu \Delta x}\left(E_z^{a+1,b} - E_z^{a,b}\right) \\ E_z^{a,b+1} &= E_z^{a,b} + \frac{\Delta t}{\epsilon \Delta x}\left(H_y^{a+1/2,b+1/2} - H_y^{a-1/2,b+1/2}\right) \end{aligned} \tag{5}$$

A good practice is to represent the update coefficients $\frac{\Delta t}{\mu \Delta x}$ and $\frac{\Delta t}{\epsilon \Delta x}$ in terms of the ratio of how the energy can propagate in a single temporal step $c\Delta t$. Defining $\epsilon = \epsilon_r \epsilon_o$, $\mu = \mu_r \mu_o$

and the Courant number $S_c = c\Delta t/\Delta x$, we can write the following relations:

$$\begin{aligned} \frac{1}{\epsilon}\frac{\Delta t}{\Delta x} &= \frac{Z_o}{\epsilon_r}S_c \\ \frac{1}{\mu}\frac{\Delta t}{\Delta x} &= \frac{1}{Z_o\mu_c}S_c \end{aligned} \tag{6}$$

where $Z_o = \sqrt{\mu_o/\epsilon_o}$ defines the free-space impedance.

An efficient spatial discretization is obtained when

$$\Delta x \approx \lambda/10, \tag{7}$$

where λ represents the smallest wavelength depending on the geometry that we are simulating and the maximal frequency. A restriction of the time step size is needed in order to ensure stable results. The condition is:

$$\Delta t \leq \frac{\Delta x}{c} \tag{8}$$

2.1 Implementation

For the implementation, the goal is to translate the update equations into a usual program. For these purposes, we will first first discard the subscripts. Moreover, time will be considered as a global variable and will be put in a single integer variable. Since we can not construct a program that explicitly uses offset of one-half (node are put in arrays and elements are specified using integer indices), we will keep in mind that the elements of the arrays E_z and H_y are offset from each other by a half spatial step even if the values of the arrays will be accessed using integer indexes. Furthermore, we will assume that an electric-field node exists to the left of the magnetic-field node with the same index. Hereafter, we will assume that the Courant number is equal to one. The update equations will then be written in the program as:

$$\begin{aligned} Hy[m] &= Hy[m] + (Ez[m+1] - Ez[m])/Z0 \\ Ez[m] &= Ez[m] + (Hy[m] - Hy[m-1]) * Z0 \end{aligned}$$

However, the "standard" updates can not be done for two special nodes:

1. $Hy[-1]$ does not exist for $Ez[0]$ in C or $Hy[0]$ does not exist for $Ez[1]$ in Matlab;

2. Element $Ez[200]$ does not exist for $Hy[199]$ in C or $Ez[201]$ does not exist for $Hy[200]$ in Matlab

To overcome this problem, we will use the absorbing boundary conditions. For sake of simplicity, we will use at first instance consider a constant impedance.

2.2 Simulation

Let first illustrate the method by considering a wave propagation in free space with 350 electrics and magnetic field nodes. The results depicted in Figure show that the output is a Gaussian. Recall that we considered $c\Delta t = \Delta x$ for this simulation, thus the fields move one step for every time step. Please note that the field is recorded at $Ez[50]$

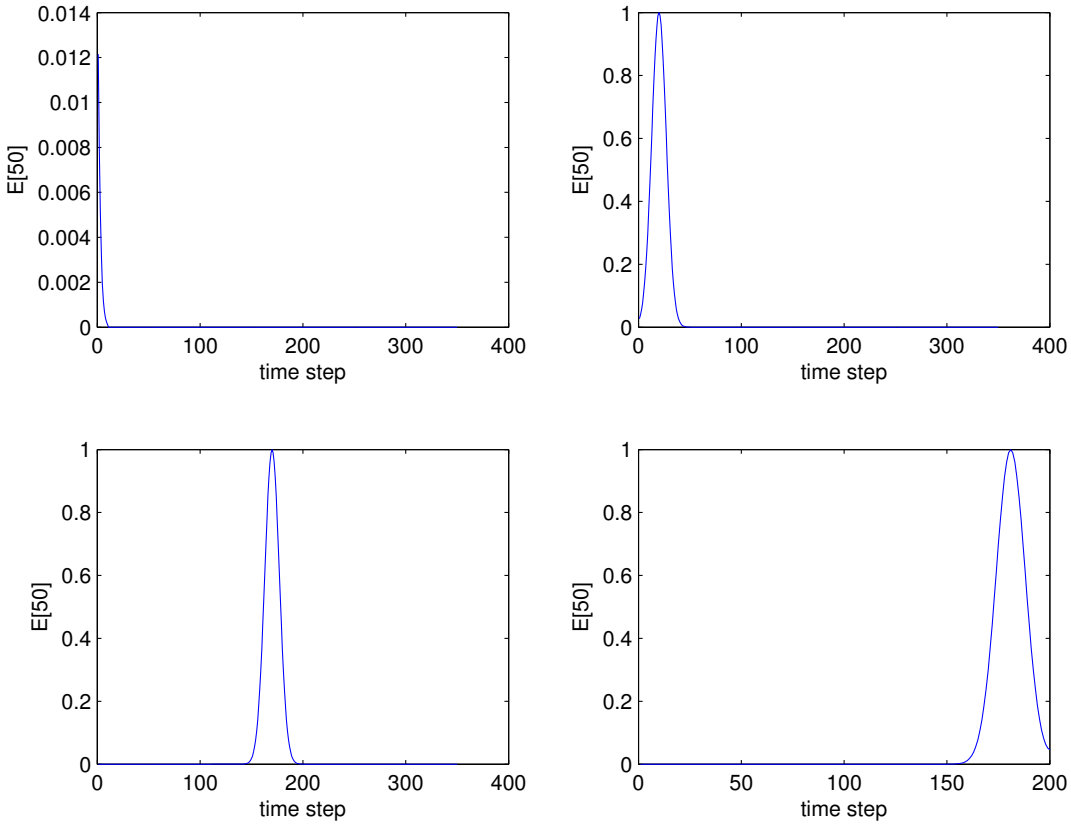

Figure 2: 1D simulation

3 The 2D FDTD algorithm

The Maxwell equations in 2D are given as follows:

$$\begin{aligned} -\sigma_m H - \mu\frac{\partial H}{\partial t} &= \frac{\partial E_z}{\partial y}\vec{1}_x - \frac{\partial E_z}{\partial x}\vec{1}_y \\ \sigma E + \epsilon\frac{\partial E}{\partial t} &= \left(\frac{\partial H_y}{\partial x} - \frac{\partial H_x}{\partial y}\right)\vec{1}_x \end{aligned} \tag{9}$$

Afterwards, the 2D Maxwell's equation are discretize in space-time in the same way as the one-dimensional, thus the following notation will be used:

$$\begin{aligned} H_x(x,y,t) &= H_x(m\Delta_x, n\Delta_x, q\Delta_y) = H_x^q[m,n] \\ H_y(x,y,t) &= H_y(m\Delta_x, n\Delta_x, q\Delta_y) = H_y^q[m,n] \\ E_z(x,y,t) &= E_z(m\Delta_x, n\Delta_x, q\Delta_y) = E_z^q[m,n] \end{aligned} \tag{10}$$

The necessary update-equations are obtained by staggering each of the field components in space. Please note that all magnetic field components can exist at the same time, i.e, the electric field must be offset from the magnetic field, but magnetic components do not necessary need to be staggered relative to each other. Using the same steps as in the 1D, the following update equations are obtained:

$$\begin{aligned} H_x^{q+1/2}[m,n+1/2] &= \frac{1-\frac{\sigma_m\Delta_t}{2\mu}}{1+\frac{\sigma_m\Delta_t}{2\mu}}H_x^{q-1/2}[m,n+1/2] - \frac{1}{1+\frac{\sigma_m\Delta_t}{2\mu}}\frac{\Delta_t}{\mu\Delta_y}(E_z^q[m,n+1] - E_z^q[m,n]) \\ H_y^{q+1/2}[m+1/2,n] &= \frac{1-\frac{\sigma_m\Delta_t}{2\mu}}{1+\frac{\sigma_m\Delta_t}{2\mu}}H_y^{q-1/2}[m+1/2,n] - \frac{1}{1+\frac{\sigma_m\Delta_t}{2\mu}}\frac{\Delta_t}{\mu\Delta_y}(E_z^q[m+1,n] - E_z^q[m,n]) \end{aligned}$$

$$E_z^{q+1/2}[m,n] = \frac{1-\frac{\sigma\Delta_t}{2\epsilon}}{1+\frac{\sigma\Delta_t}{2\epsilon}} + \frac{1}{1+\frac{\sigma\Delta_t}{2\epsilon}}(X-Y)$$

$$\text{where :} \quad \begin{cases} X = \frac{\Delta_t}{\epsilon\Delta_x}H_y^{q+1/2}[m+1/2,n] - \frac{\Delta_t}{\epsilon\Delta_x}H_y^{q+1/2}[m-1/2,n] \\ Y = \frac{\Delta_t}{\epsilon\Delta_y}H_x^{q+1/2}[m,n+1/2] - \frac{\Delta_t}{\epsilon\Delta_y}H_x^{q+1/2}[m,n-1/2] \end{cases}$$

As in the 1D case, these three equations put in appropriate loops, constitute the main machinery of the two-dimensional FDTD. Please note that the time step condition is more severe for the 2D FDTD to ensure stable results:

$$\Delta t \leq \frac{\Delta x}{c\sqrt{2}} \tag{11}$$

In practice many obstacles are placed in front of wave sources like GSM antennas, Radio antennas and others. These phenomenons are suffering diffraction as well as reflection and

refraction. Thenceforth in order to validate the FDTD method, a few simulations will be done.

3.1 Simulations

3.1.1 Knife-edge model

The Knife-edge model is a diffraction model often used to simulate diffraction of a wave source placed behind a semi-infinite and perfectly conductor plane. This plane is simulated below considering that the field is equal to zero in the plane.

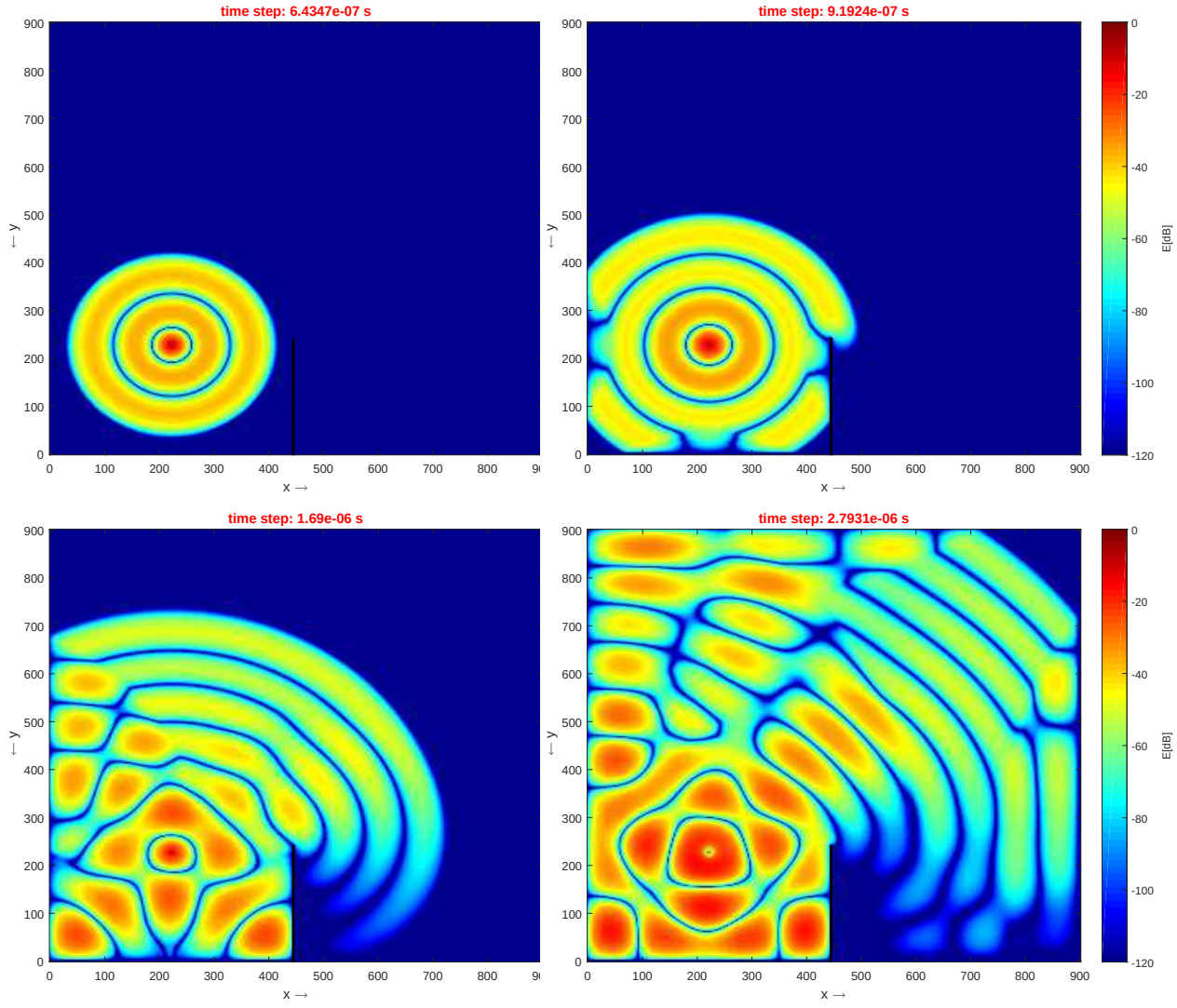

Figure 3: Knife-edge model experiment

As shown on the different figures 3 the wave is propagating and there is reflection on the plane. The wave is interfering right after the plane and there are some area that is not covered by the wave of the antenna.

3.1.2 Specific absorption rate (SAR) study

In this simulation, the power absorbed by the human tissues for a given emitted is calculated. The specific absorption rate gives the amount of power lost inside the tissues. The SAR is given in W/kg (SI: $m^2 * s^{-3}$):

$$SAR = \frac{1}{m} \int_D \frac{|E_z|^2}{2} dV, \tag{12}$$

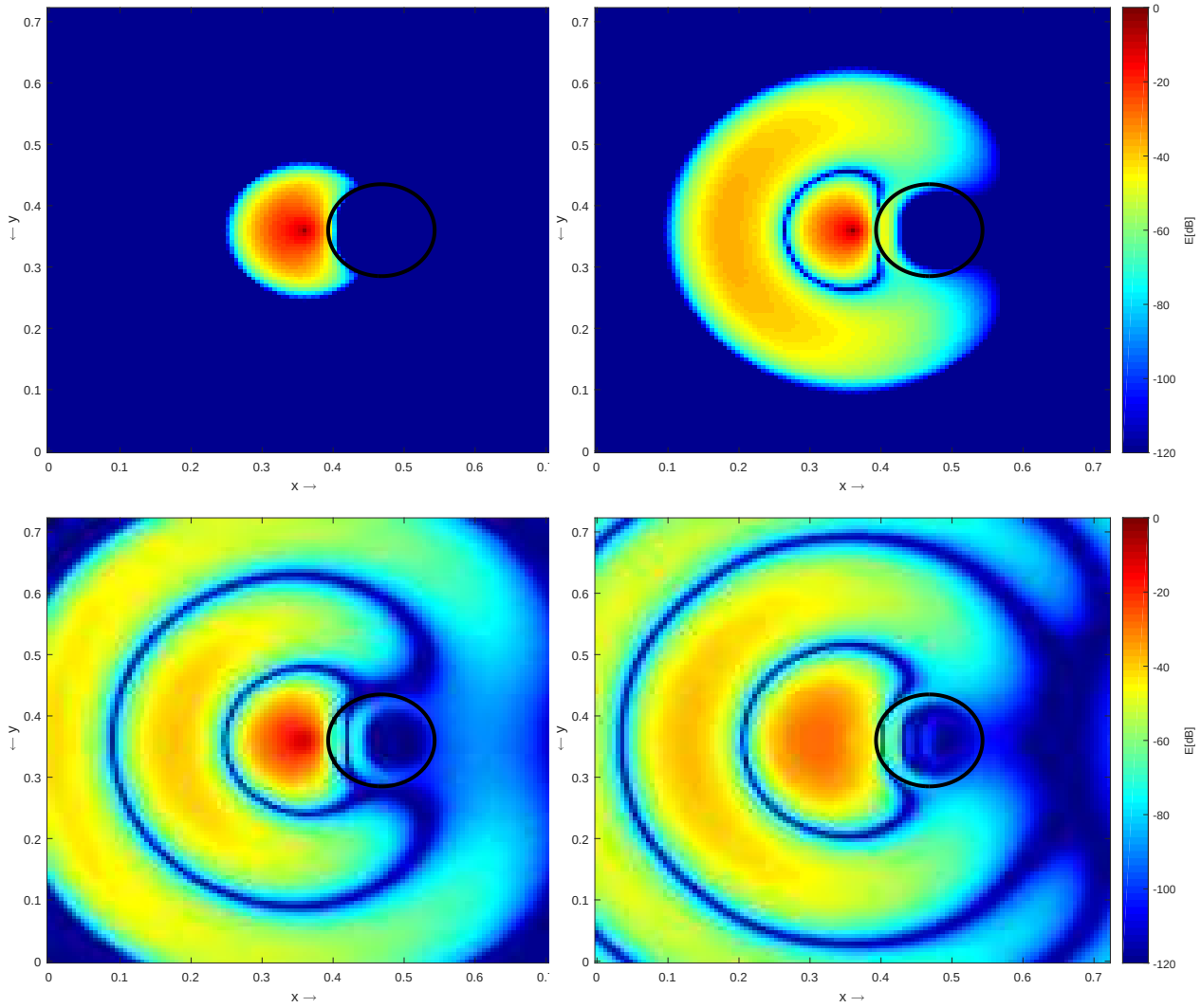

Figure 4: SAR experiment on the head of an adult

In this experiment, we simulate a source emitting at the operating GSM frequency 915 MHz. The source is a simple sinusoid. The human head is simulated by a circle. The step in x and y are chosen as $\lambda/10$ in order to obtain a step size of 1 meter. The skull permittivity and conductivity are 43 and 1.3 respectively.As shown on Figure 4 the wave passes through the skull.

The SAR in this situation is equal for the first figure($8.02.10^{-8}$ seconds) to $7.42.10^{-7}$ W/kg. Typically the limit value for SAR in the European union is equal to 2 W/kg [1]. Afterwards, we put a metal between the head and the source and we compare the results. An interesting case would be to vary the radius of the skull and taking a smaller one like the radius of a 5 years old baby. The skull in this case has a radius of approximately 7.5 cm.[2]

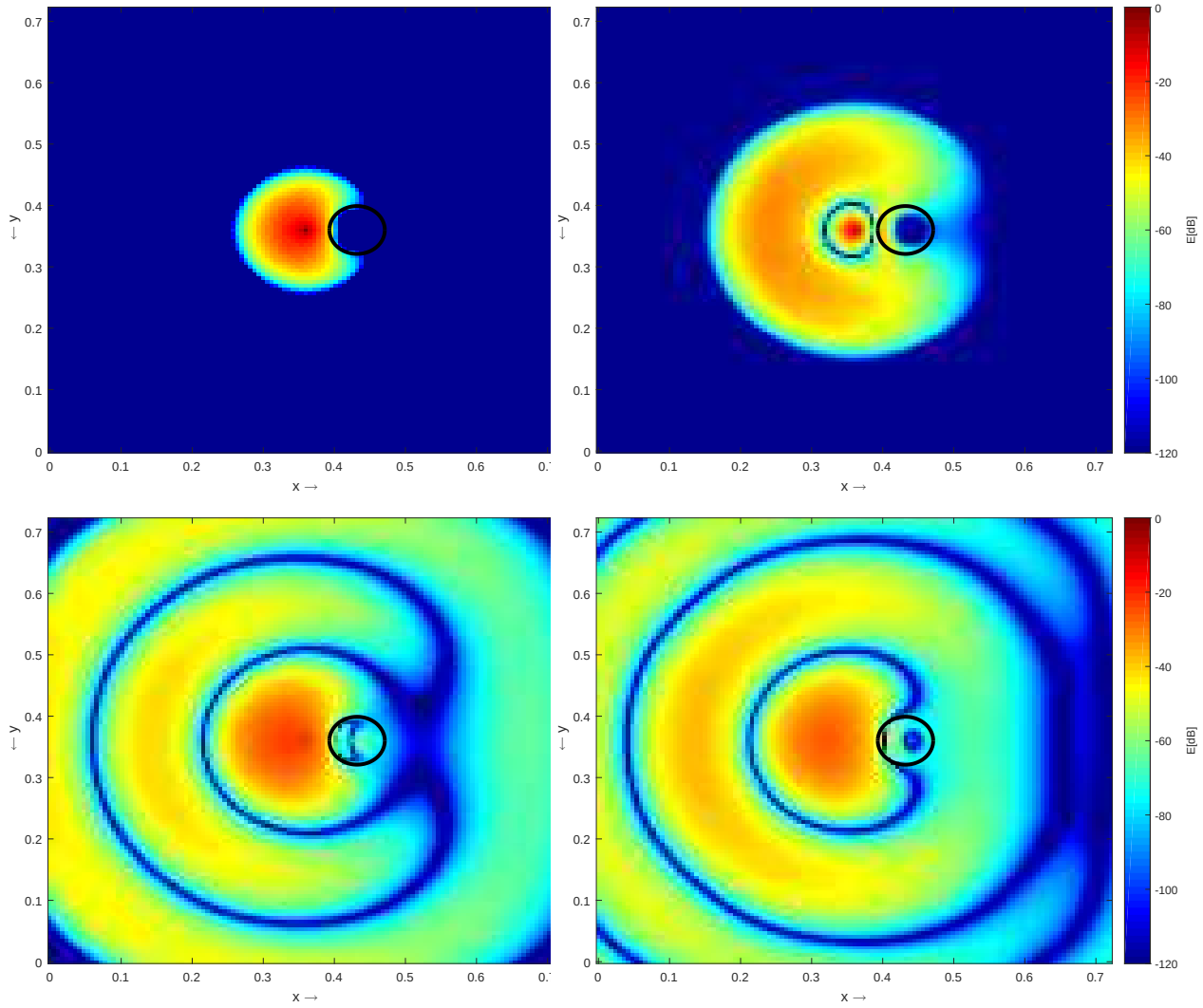

Figure 5: SAR experiment on the head of a baby

As it can be noticed on the Figures above, the wave penetrates more in the head of a baby than in the head of a grown-up person. This can be explained by the little radius of the head of a baby. The SAR in this condition of experiment is equal to $3.08.10^{-6}$ W/kg after a time of $2.4.10^{-6}$ seconds.

[1] International Electrotechnical Commission: *https* : *//webstore.iec.ch/publication/*6588

[2] National Center for Health Statistics:*http* : *//www.cdc.gov/growthcharts/html*$_c$*harts/hcageinf.htm*

3.1.3 Specific absorption rate (SAR) with metal

As it can be seen on the next Figures, when a metal plate is put in front of the skull, there is more attenuation of the incident wave. The metal part is a little bit protecting the head of the person. This can be explained by the conductivity property of the metal. Indeed, the metal being a good conductor it is therefore more reflecting the incident waves on the head.

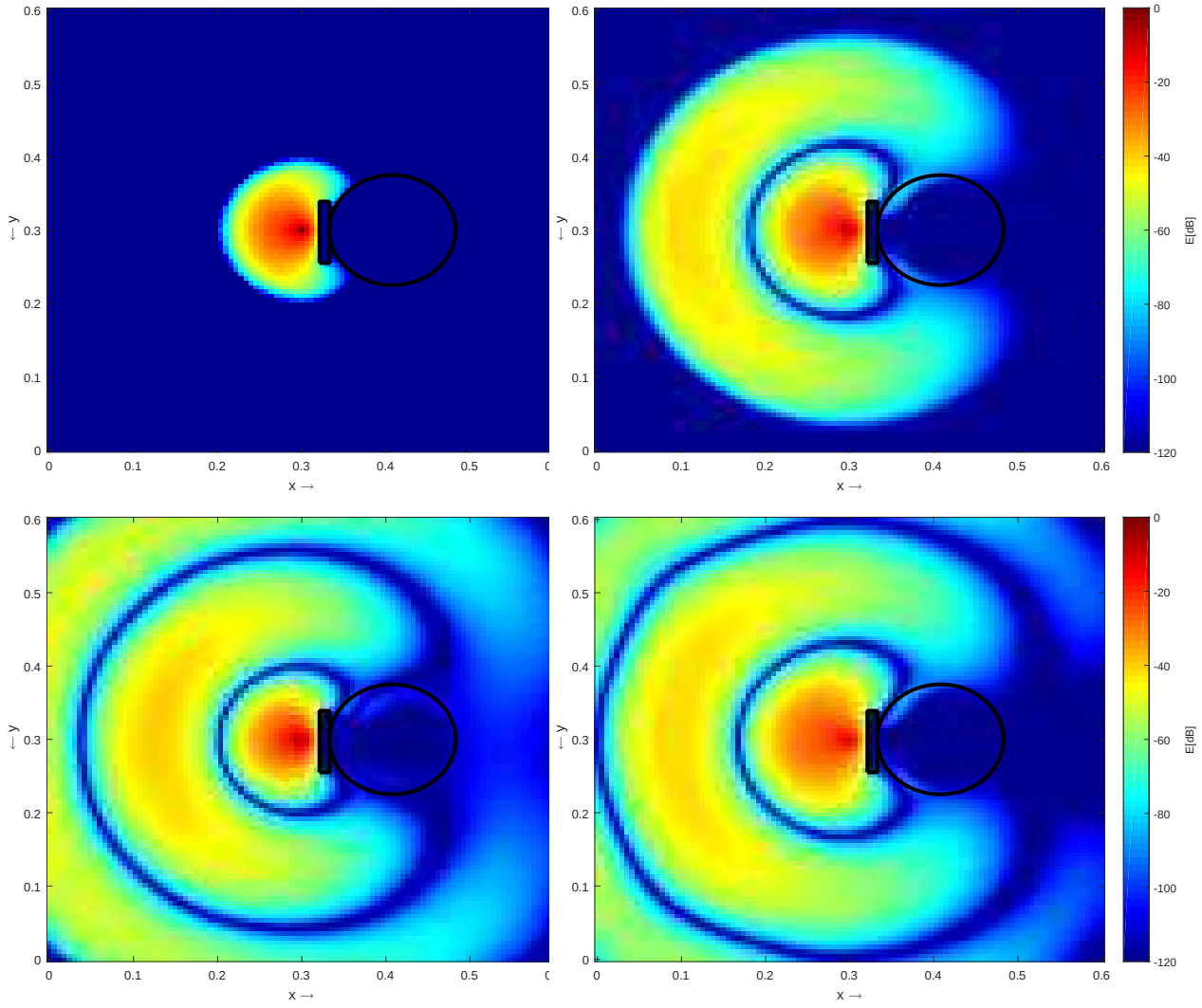

Figure 6: SAR experiment with metal on the head of adult adult

In the Figure corresponding to the plot with a adult head, it can clearly be noticed that the metal part is attenuated more than the case without medal part.

As for the plot with a baby head, the SAR for the last figure is equal to $2.0796.10^{-5}$ W/kg. We see if we compare with the value without the metal part that there is little more attenuation with the metal part.

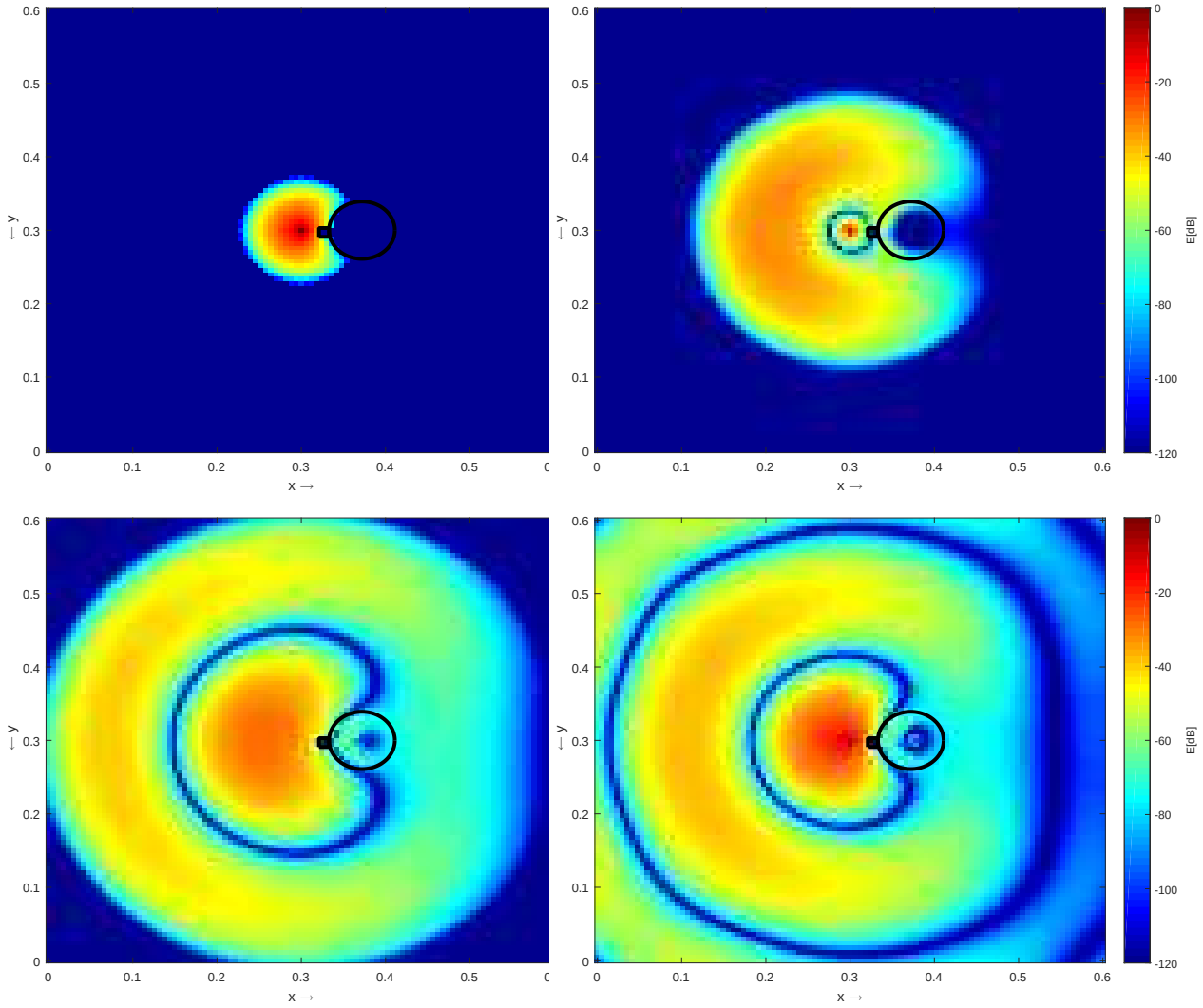

Figure 7: SAR experiment with metal on the head of a baby

3.1.4 Young Two-Slit Experiment

This experiment was first conducted by Thomas Young at the beginning of the 19^{th} century and consisted in putting a barrier cut in two places in front of a source of light. This experiment was conducted to demonstrate the wave behaviour of the light. In our case, the source is a sinusoid of frequency f:

$$\text{source} = \sin(2\pi(n-1)f\delta t) \tag{13}$$

In this experiment, two very narrow parallel slits, separated by a distance d, are cut into a thin sheet of metal as depicted in Figure 8. The result of the simulation is shown in Figure 8

As shown on the Figure 8 the waves are merging together and interfering either in a additive way or a substractive way to produce. The region where happens the constructive interference

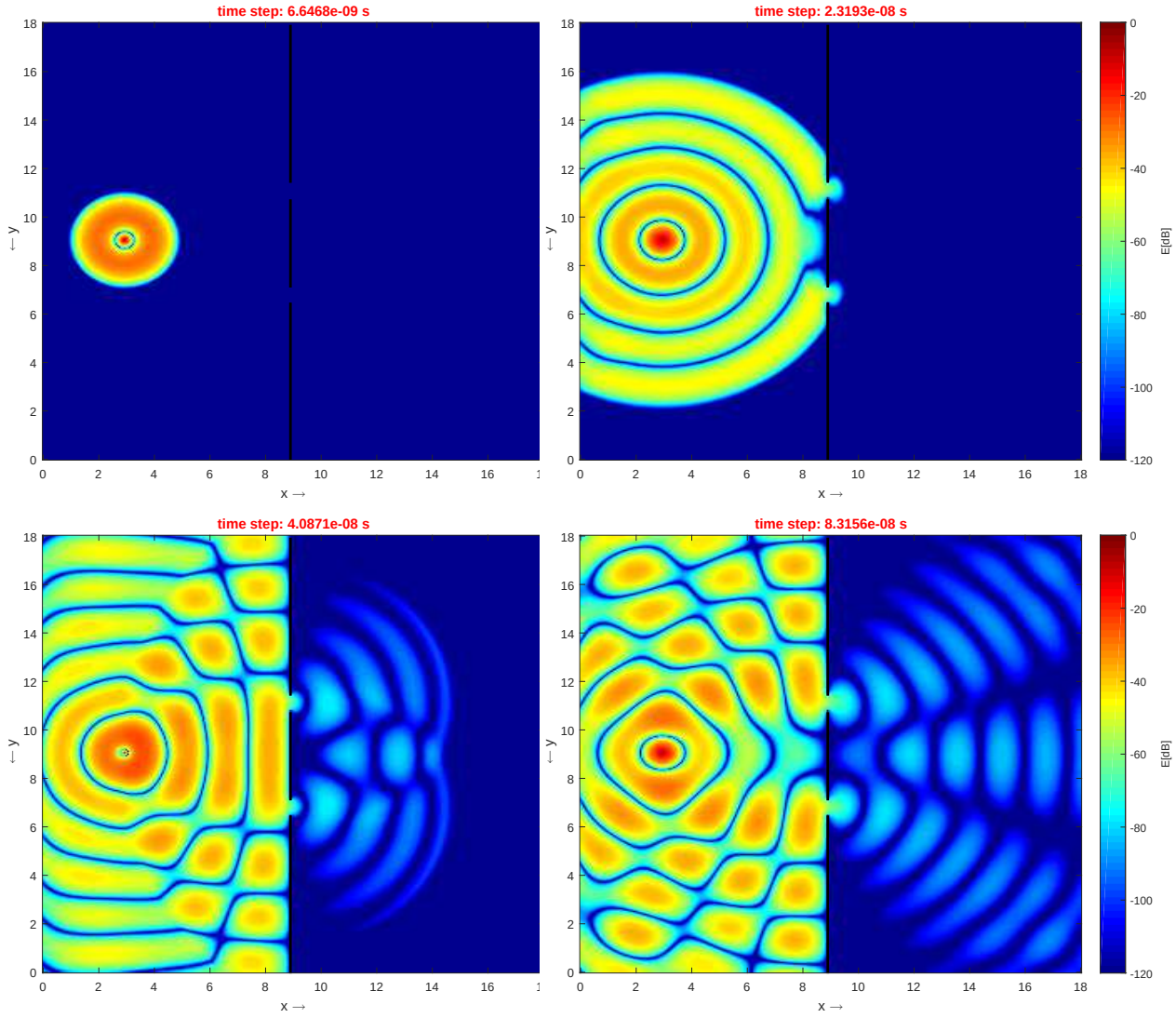

Figure 8: Young experiment

are the region with the highest value in power (see Figure 8). In these regions the waves are in phase and sum up together. On the contrary, the destructive interference are the region with the lowest value in power as it is in those regions that the waves are cancelling each other. This phenomenon happens when the waves are phase shifted and the phase shift is the result of the diffraction of the incident wave in both holes.

4 Conclusion

The implementation and simulation of a two-dimensional Finite-Difference Time-Domain method algorithm have been done.The different simulations allowed us to put in practice different scenarios related to wave behaviour. The reality has been simulated taking into account different boundary conditions for different situations. In all the simulations, the

source is a sinusoid that puts the energy into the system. The absorbing boundary conditions are taken into account, so that the field is zero at the boundaries. The obtained results show the robustness of the FDTD method whether in 1D case or 2D case. This also helped us to understand better the reality of the propagation of wave.